MRI and ^{18}FET-PET Predict Survival Benefit from Bevacizumab Plus Radiotherapy in Patients with Isocitrate Dehydrogenase Wild-type Glioblastoma: Results from the Randomized ARTE Trial

Hans-Georg Wirsching[1], Ulrich Roelcke[2], Jonathan Weller[1], Thomas Hundsberger[3], Andreas F. Hottinger[4], Roger von Moos[5], Francesca Caparrotti[6], Katrin Conen[7], Luca Remonda[8], Patrick Roth[1], Adrian Ochsenbein[9], Ghazaleh Tabatabai[1], and Michael Weller[1]

ABSTRACT

Purpose: To explore a prognostic or predictive role of MRI and O-(2–^{18}F-fluoroethyl)-L-tyrosine (^{18}FET) PET parameters for outcome in the randomized multicenter trial ARTE that compared bevacizumab plus radiotherapy with radiotherpay alone in elderly patients with glioblastoma.

Patients and Methods: Patients with isocitrate dehydrogenase wild-type glioblastoma ages 65 years or older were included in this *post hoc* analysis. Tumor volumetric and apparent diffusion coefficient (ADC) analyses of serial MRI scans from 67 patients and serial ^{18}FET-PET tumor-to-brain intensity ratios (TBRs) from 31 patients were analyzed blinded for treatment arm and outcome. Multivariate Cox regression analysis was done to account for established prognostic factors and treatment arm.

Results: Overall survival benefit from bevacizumab plus radiotherapy compared with radiotherapy alone was observed for larger pretreatment MRI contrast-enhancing tumor [HR per cm^3 0.94; 95% confidence interval (CI), 0.89–0.99] and for higher ADC (HR 0.18; CI, 0.05–0.66). Higher ^{18}FET-TBR on pretreatment PET scans was associated with inferior overall survival in both arms. Response assessed by standard MRI-based Response Assessment in Neuro-Oncology criteria was associated with overall survival in the bevacizumab plus radiotherapy arm by trend only ($P = 0.09$). High ^{18}FET-TBR of noncontrast-enhancing tumor portions during bevacizumab therapy was associated with inferior overall survival on multivariate analysis (HR 5.97; CI, 1.16–30.8).

Conclusions: Large pretreatment contrast-enhancing tumor mass and higher ADCs identify patients who may experience a survival benefit from bevacizumab plus radiotherapy. Persistent ^{18}FET-PET signal of no longer contrast-enhancing tumor after concomitant bevacizumab plus radiotherapy suggests pseudoresponse and predicts poor outcome.

Introduction

Glioblastoma is an invariably fatal disease with a median overall survival in the range of 1 year (1). The proliferation of hyperplastic, dysfunctional blood vessels is a histologic hallmark of glioblastoma (2). VEGF A, a key driver of angiogenesis in glioblastoma and other cancers, can be targeted with the VEGF-neutralizing antibody bevacizumab (3). Definitive FDA approval of bevacizumab for the treatment of recurrent glioblastoma was based on prolonged progression-free survival (PFS) and apparent clinical benefit (4–6). However, randomized clinical trials of bevacizumab in patients with newly diagnosed or recurrent glioblastoma failed to demonstrate prolonged overall survival (6–8).

Pretreatment MRI parameters, including absence of imaging necrosis or higher apparent diffusion coefficients (ADCs), may identify subgroups of patients with overall survival benefit from bevacizumab in recurrent glioblastoma (9–11). How to optimally monitor patients with glioblastoma treated with bevacizumab remains a matter of debate, because contrast enhancement on T1-weighted MRI sequences—the key parameter to monitor glioblastoma growth in classical response criteria (12, 13)—may decrease within days after implementation of antiangiogenic therapy and often reflects restoration of blood–brain barrier function rather than tumor shrinkage (14–16). This phenomenon has been termed *pseudoresponse* (17) and may account for unrecognized disease progression in patients on antiangiogenic therapy, leading to deferred salvage therapy and potentially even shorter overall survival.

The Response Assessment in Neuro-Oncology (RANO) working group has incorporated clinical parameters and T2-weighted MRI sequences as measures to address the challenges of misleading treatment-induced contrast enhancement dynamics (12). There is, however, large interobserver variability regarding the time point of progression by RANO (18) and in bevacizumab-treated patients, response by RANO may not predict overall survival in patients with newly diagnosed (19) or recurrent glioblastoma (20).

[1]Department of Neurology, University Hospital and University of Zurich, Zurich, Switzerland. [2]Department of Neurology, Cantonal Hospital Aarau, Aarau, Switzerland. [3]Department of Neurology, Cantonal Hospital St. Gallen, St. Gallen, Switzerland. [4]Departments of Clinical Neurosciences and Medical Oncology, University Hospital Lausanne, Lausanne, Switzerland. [5]Department of Medical Oncology, Cantonal Hospital Graubuenden, Chur, Switzerland. [6]Department of Radiation Oncology, University Hospital Geneva, Geneva, Switzerland. [7]Department of Medical Oncology, University Hospital Basel, Basel, Switzerland. [8]Department of Neuroradiology, Cantonal Hospital Aarau, Aarau, Switzerland. [9]Department of Medical Oncology, Inselspital, Berne University Hospital, University of Berne, Berne, Switzerland.

Note: Supplementary data for this article are available at Clinical Cancer Research Online (http://clincancerres.aacrjournals.org/).

Clinicaltrials.gov identifier: NCT01443676.

Corresponding Author: Hans-Georg Wirsching, University Hospital of Zurich, Frauenklinikstr. 26, Zurich 8006, Switzerland. Phone: +41-44-255-5500; Fax: +41-44-255-4380; E-mail: hans-georg.wirsching@usz.ch

Clin Cancer Res 2021;27:179–88

doi: 10.1158/1078-0432.CCR-20-2096

Translational Relevance

Response assessment of patients with brain tumors exposed to antiangiogenic therapy remains challenging because reduction of contrast enhancement on MRI may reflect blood–brain barrier restoration rather than tumor regression, a phenomenon termed pseudoresponse. The Response Assessment in Neuro-Oncology (RANO) working group supports the use of amino acid PET to monitor noncontrast-enhancing tumor growth in bevacizumab-treated patients based on limited evidence. We herein report the MRI/PET substudy of a randomized, clinically and molecularly well-annotated multicenter cohort of isocitrate dehydrogenase wild-type patients with glioblastoma treated with or without bevacizumab. Our exploratory analyses suggest that larger pretreatment contrast-enhancing tumor volume and low ^{18}FET intensity of noncontrast-enhancing tumor during bevacizumab treatment may predict survival benefit from bevacizumab plus radiotherapy. MRI response by RANO was only by trend associated with overall survival in bevacizumab-treated patients. Our study supports the use of ^{18}FET intensity in noncontrast-enhancing tumor to identify pseudoresponse in patients with glioblastoma treated with antiangiogenic agents.

PET utilizing the amino acid tracers O-(2–^{18}F-fluoroethyl)-L-tyrosine (^{18}FET) or (S-^{11}C-methyl)-L-methionine (^{11}C-MET) can be utilized to differentiate viable glioma tissue from treatment-induced changes with high sensitivity and specificity (21). Uncontrolled studies suggest that ^{18}FET-PET may detect tumor progression during antiangiogenic treatment earlier than MRI (20, 22, 23). This led the RANO working group to incorporate recommendations for the use of amino acid PET in the response assessment of such patients (24).

The randomized multicenter open-label phase II trial ARTE explored the efficacy of bevacizumab as an adjunct to hypofractionated radiotherapy in elderly patients (>65 years) with newly diagnosed glioblastoma (25). Here we report associations of serial MRI and ^{18}FET-PET parameters with benefit from bevacizumab plus radiotherapy in this clinically and molecularly homogenous, well-annotated cohort of patients with glioblastoma.

Patients and Methods

Study design

ARTE was a 2:1 randomized phase II clinical trial of hypofractionated radiotherapy of 15 × 2.66 = 40 Gy in combination with bevacizumab 10 mg/kg bodyweight administered every 2 weeks compared with hypofractionated radiotherapy alone in elderly (>65 years) patients with newly diagnosed glioblastoma. Here we analyzed associations of pretreatment and follow-up imaging parameters by treatment arm with outcome. Patients with isocitrate dehydrogenase (IDH)-mutant glioblastoma or alternative diagnoses by central pathology review were excluded from this analysis. Outcome measures were PFS from randomization and overall survival from histologic diagnosis. The ARTE trial and *post hoc* translational analyses were approved by the local ethical committee (KEK-ZH No. 2011–0135) and were conducted in accordance with the Declaration of Helsinki and its amendments. All patients gave written informed consent prior to inclusion. The ARTE trial is registered at clinicaltrials.gov (NCT01443676).

Molecular analyses

Analysis of the promoter methylation status of the O^6-methylguanine DNA methyltransferase (*MGMT*) promoter region was done in all patients and a methylated *MGMT* promoter became an exclusion criterion by amendment (November 2013) when it became clear that patients with tumors with a methylated *MGMT* derived larger benefit from temozolomide monotherapy than from radiotherapy alone (26, 27). *MGMT* promoter methylation status was determined by methylation-specific PCR (28). *IDH* mutation status was determined by IHC (29) or sequencing of *IDH1* and *IDH2*. Genome-wide CpG methylation was determined by 450k array profiling and classified utilizing a publicly available tool (www.molecularneuropathology.org; ref. 30). Genomic copy-number alterations were derived from methylation arrays and subtypes annotated manually according to prognostic subgroups (31). Gene expression subtypes were determined utilizing the nCounter gene expression platform (NanoString Technologies) to assess a custom gene set for subsequent classification based on published centromeres (32, 33).

MRI and ^{18}FET-PET parameters

Pretreatment MRI and ^{18}FET-PET were performed postoperatively within 10 days before the start of study treatment, bevacizumab plus radiotherapy or radiotherapy alone. Follow-up scans were to be acquired 4 weeks after completion of radiotherapy (week 7) and at least every 3 months thereafter until progression. MRI was done according to local investigators' protocols on 1.5 T or 3 T scanners. Gadolinium was used as contrast agent. The slice thickness was at the most 3 mm for any sequences analyzed. There was no centralized specification of echo or repetition times or of field-of-view values. MRI included contrast enhancement and T2 as the minimum set of sequences for volumetric characterization and response assessment. Pretreatment necrosis was defined as hyperintensity on T2 and hypointensity on T1 located within contrast enhancement. Diffusion-weighted sequences were expressed by mean ADC in absolute units of 10^{-3}mm^2/s. ADC$_L$, the mean of the lower distribution of a double Gaussian model, was also determined. Fractional anisotropy was not reported. Pretreatment contrast-enhancing and T2 volumes were determined utilizing the Brainlab Elements version 2.6 software (Brainlab). Treatment response for MRI sequences was determined according to RANO criteria by measuring perpendicular tumor diameters to yield bidimensional tumor size estimates in mm^2 and taking the clinical course into account (12). Tumor size changes during follow-up were calculated as percent change from pretreatment scans. Static ^{18}FET-PET scans were acquired 30 to 50 minutes after tracer injection. A standardized imaging acquisition protocol for MRI and PET scans was implemented in all centers participating in the ARTE trial.

Both ADC values and ^{18}FET intensity values were also measured separately for nonenhancing and for enhancing tumor to account for different diffusion properties and passive tracer diffusion (34). Diffusion-weighted MRI and PET images were fused with contrast-enhancing MRI. Noncontrast-enhancing tumor was defined by T2 hyperintensity in the absence of contrast enhancement, that is, including areas of potential vasogenic edema. PET region-of-interest (ROI) analysis was done outlining the respective tumor compartments on the superimposed MRI and PET images. ROI were determined in two perpendicular planes, each in the slice with the maximum tumor area. For ^{18}FET intensity quantification, tumor-to-brain ratios (TBR) were determined by dividing the mean tumor ROI intensity values on the plane with the largest tumor area on MRI by the mean intensity in a

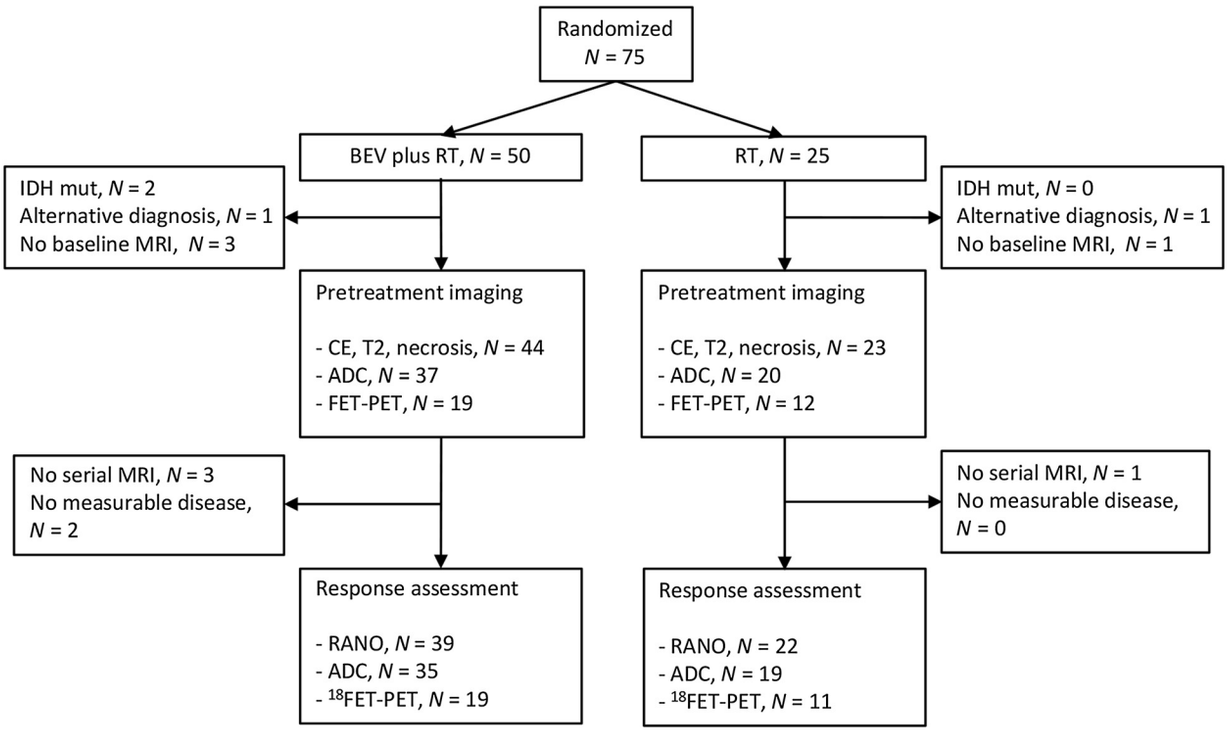

Figure 1.

Study population. ADC, apparent diffusion coefficients; BEV plus RT, bevacizumab in combination with hypofractionated radiotherapy; CE, contrast enhancement on T1-weighted MRI sequences; ^{18}FET-PET, O-(2–^{18}F-fluoroethyl)-L-tyrosine positron emission tomography; IDH, isocitrate dehydrogenase; MRI, magnetic resonance imaging; RANO, response assessment in neuro-oncology working group criteria; RT, radiotherapy alone.

ROI on the plane with the largest cerebellar diameter as the reference (35). Analyses of imaging parameters were done centrally by U. Roelcke and J. Weller blinded for treatment arm and outcome.

Statistical methods

The χ^2 test was applied to compare categorical variables and the Mann–Whitney *U* test was applied for continuous variables. ROC curve analyses utilizing median overall survival to determine prognostic cut-offs were done to segregate patients by continuously scaled imaging parameters. Best response was computed as time-dependent covariate as indicated. Treatment arms and indicated subgroups were compared in exploratory analyses with respect to PFS and overall survival using the log-rank test, or univariate and multivariate Cox proportional hazards models incorporating indicated covariates. Age and Karnofsky performance score (KPS) were dichotomized at established cut-offs (age: 71 years or more vs. 65–70 years, KPS: <90% vs. 90%–100%; ref. 25). No correction for multiple testing was done in this exploratory analysis. *P* values below 0.05 were considered statistically significant.

Results

Study population

The primary analysis population is detailed in **Fig. 1**. Of 75 patients enrolled, 50 were treated with bevacizumab plus radiotherapy and 25 with radiotherapy alone. Eight patients were excluded from subsequent analyses, two in the bevacizumab plus radiotherapy arm with mutated IDH, one patient in each arm with an alternative diagnosis on central pathology review, and four patients without pretreatment MRI available. Longitudinal volumetric analyses of contrast-enhanced and T2-weighted MRI sequences were available from 44 and 23 patients, ADC from 37 and 20 patients, and ^{18}FET-TBR from 19 and 12 patients, in the bevacizumab plus radiotherapy and radiotherapy arms. Demographic, clinical, and molecular characteristics at baseline were balanced between arms, including age, sex, contrast-enhancing tumor volume, KPS, steroid use, *MGMT* promoter methylation status, genome methylation subtypes, and gene expression subtypes in the overall cohort (25), and in the subcohorts with available MRI and FET-PET studied here (**Table 1**; Supplementary Table S1).

Pretreatment contrast enhancement and ADC are associated with overall survival benefit from bevacizumab plus radiotherapy

ROC curve analyses identified a pretreatment contrast enhancement cut-off at 3.1 cm^3 that was associated with overall survival by trend in the bevacizumab plus radiotherapy arm (**Fig. 2A**) and at 5.3 cm^3 that segregated patients by overall survival in the radiotherapy arm (**Fig. 2B**). Analyzing contrast-enhancing volumes as continuous variable confirmed that larger pretreatment contrast-enhancing volume was associated with inferior overall survival in both treatment arms. This association was less pronounced in the bevacizumab plus radiotherapy arm than in the radiotherapy arm, suggesting that a negative association of contrast enhancement with overall survival is in part abrogated by bevacizumab. Along the same lines, there was an interaction of pretreatment contrast enhancement with treatment arm indicating preferential benefit from bevacizumab plus radiotherapy in tumors with larger contrast-enhancing volumes (**Fig. 2C**).

Table 1. Patient characteristics at baseline.

	BEV plus RT $N = 44$	RT $N = 23$	*P*
Age, years			
Median	70	69	
Range	65–87	65–79	0.62
Sex, *N* (%)			
Male	25 (57)	11 (48)	
Female	19 (43)	12 (52)	0.48
Tumor volume, cm^{3a}			
Median	3.5	1.1	
Range	0.0–54.1	0.5–40.0	0.35
KPS, *N* (%)			
90–100	22 (50)	15 (65)	
70–80	18 (41)	6 (26)	
60	4 (9)	2 (9)	0.46
Steroids, *N* (%)			
Yes	21 (49)	11 (48)	
No	22 (51)	12 (52)	0.94
No data	1	0	
MGMT promoter, *N* (%)			
Methylated	8 (19)	6 (27)	
Unmethylated	34 (81)	16 (73)	0.45
No data	2	1	
Gene methylation class, *N* (%)			
Receptor tyrosine kinase I	11 (31)	5 (28)	
Receptor tyrosine kinase II	15 (43)	8 (44)	
Mesenchymal	8 (23)	5 (28)	
Oncogene *MYCN*-driven	1 (3)	0 (0)	0.88
No data	9	5	
Gene expression subtype, *N* (%)			
Proneural	8 (25)	6 (38)	
Classical	11 (34)	8 (50)	
Mesenchymal	13 (41)	2 (12)	0.14
No data	12	7	

Abbreviations: BEV, bevacizumab; CL, classical; KPS, Karnofsky performance score; RT, radiotherapy.
[a]Defined as contrast-enhancing lesions on T1-weighted images.

No associations with overall survival in either treatment arm were identified for pretreatment volumetric analyses of T2-weighted images (Supplementary Fig. S1A–S1C), or of fluid attenuated inversion recovery sequences (not shown). Similar analyses were done utilizing cut-offs of pretreatment contrast enhancement and T2 volumes with respect to PFS, but we identified no interactions with PFS benefit from bevacizumab plus radiotherapy (Note S1; Supplementary Fig. S2).

We also explored whether imaging necrosis—an MRI surrogate for tumor hypoxia—was associated with overall survival. Necrosis was present in 38 of 67 patients (57%) on pretreatment MRI scans and presence of any necrosis was associated with inferior outcome (Supplementary Fig. S3A), but there was no association with benefit from bevacizumab with respect to overall survival (Supplementary Fig. S3B) or PFS (not shown).

ADC values were analyzed in contrast-enhancing tumor portions and cut-offs to segregate patients by high versus low mean ADC values were defined by ROC curve analyses. In the bevacizumab plus radiotherapy arm, pretreatment ADC values above 1.19 mm^2/second were associated with longer overall survival (**Fig. 2D**), but no such association was detected in the radiotherapy arm (**Fig. 2E**). There was a marked interaction of pretreatment ADC with treatment arm indicating preferential overall survival benefit from bevacizumab plus radiotherapy in tumors with higher ADC (**Fig. 2F**). A similar interaction of higher ADC values in contrast-enhancing tumor portions with preferential benefit from bevacizumab plus radiotherapy was also observed with respect to PFS (Supplementary Fig. S3C).

Pretreatment ^{18}FET intensity in contrast-enhancing tumor tissue is associated with inferior overall survival independent of treatment

In contrast-enhancing tumor portions, ^{18}FET may enrich due to passive tracer diffusion in addition to active uptake by tumor cells (34), thus requiring the separate analysis of ^{18}FET intensities in contrast-enhancing and noncontrast-enhancing tumor portions. Applying ROC cut-offs of pretreatment ^{18}FET intensity in contrast-enhancing tumor lesions identified a marked association of higher ^{18}FET-TBR with inferior overall survival in the bevacizumab plus radiotherapy arm (**Fig. 2G**) and by trend in the radiotherapy arm (**Fig. 2H**), but there was no specific overall survival benefit from bevacizumab plus radiotherapy among patients with high or low ^{18}FET intensity (**Fig. 2I**). We compared the association of pretreatment contrast-enhancing volume, ADC and ^{18}FET intensity TBR with overall survival in a multivariable model that included all three parameters and correction variables for study arm interactions of ADC and contrast-enhancing volumes (Supplementary Table S2). In this model, high versus low ^{18}FET intensity was negatively associated with overall survival [hazard ratio 3.54; 95% confidence interval (CI), 1.12–11.16; $P = 0.031$], but not contrast-enhancing volumes ($P = 0.39$) or ADC ($P = 0.79$), suggesting that pretreatment ^{18}FET intensity in contrast-enhancing tumor portions may reflect prognosis more accurately than MRI-based imaging alone.

In noncontrast-enhancing tumor areas, pretreatment ^{18}FET intensity TBR were similar to normal brain (not shown), suggesting that pretreatment T2 hyperintensity may comprise mostly vasogenic edema and gliosis rather than metabolically active tumor cells. Consequently, no associations with overall survival were identified for pretreatment ^{18}FET intensity in noncontrast-enhancing tumor portions (not shown). No associations of ^{18}FET intensity TBR with PFS were identified in contrast-enhancing or noncontrast-enhancing tumor areas (not shown), suggesting that the observed association of pretreatment ^{18}FET PET with overall survival is treatment independent.

Imaging response assessment by RANO is only weakly associated with overall survival in bevacizumab-treated patients

Antiangiogenic treatment often induces a reduction in contrast enhancement that may occur within days from the initiation of therapy. This phenomenon does not necessarily reflect a reduction in tumor burden but rather restoration of blood–brain barrier function (17). One objective of the RANO criteria was to expand criteria for differentiating a definition of imaging response and tumor progression and antiangiogenic treatment beyond contrast-enhancing tumor, taking clinical and T2-weighted MRI parameters into account (12). In the ARTE trial, response by RANO computed as time-dependent variable was only by trend associated with longer overall survival in the bevacizumab plus radiotherapy arm whereas there was a clear segregation by overall survival in the radiotherapy arm (**Fig. 3A** and **B**). Utilizing the percent changes between best response and pretreatment value in contrast-enhancing volume estimates, we identified response cut-offs that were associated with overall survival in either treatment arm, albeit the segregation by contrast-enhancing response was less pronounced in the bevacizumab plus radiotherapy arm

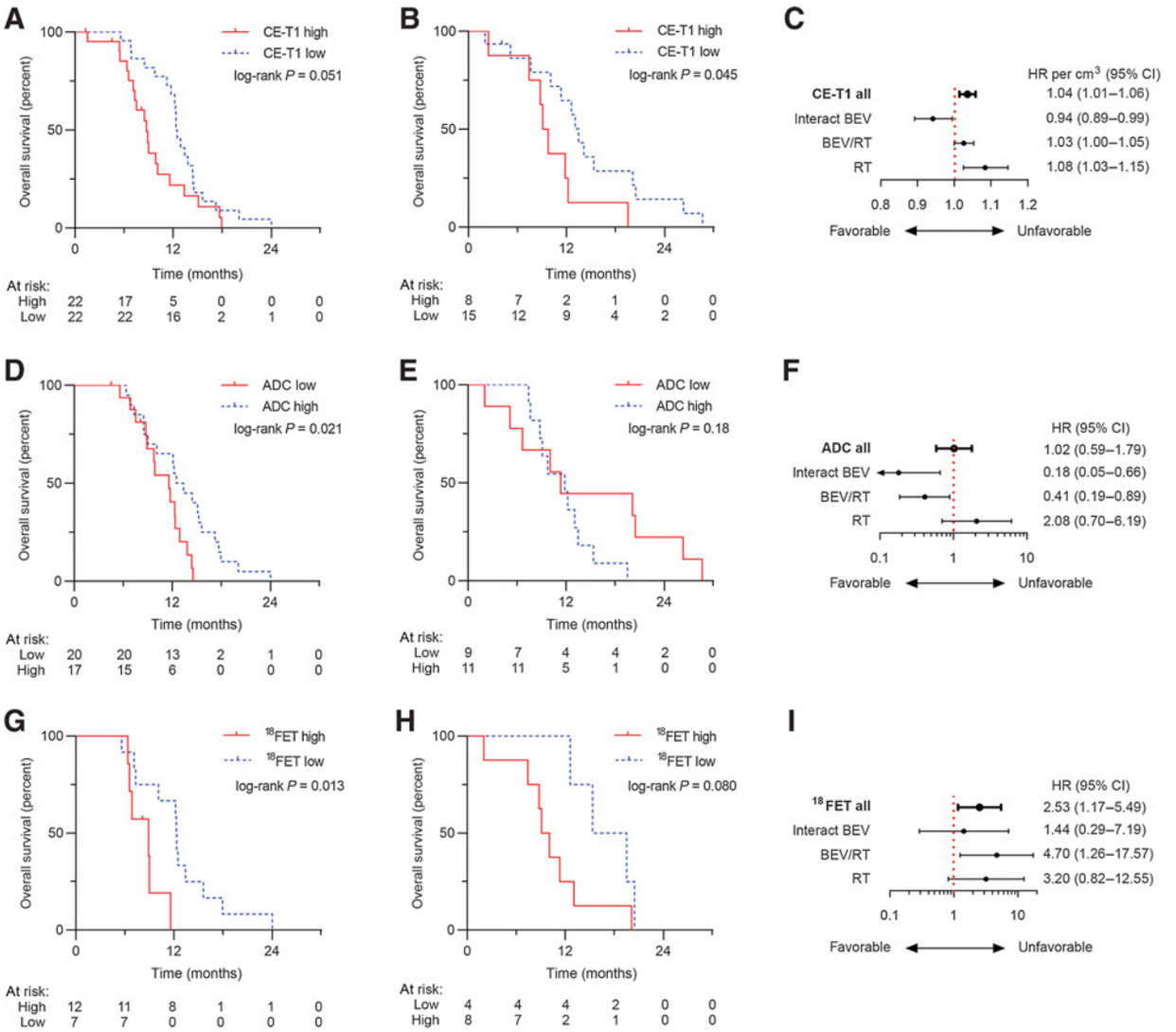

Figure 2.

Overall survival by pretreatment MRI parameters. Overall survival was analyzed by contrast-enhancing volumes (CE-T1; **A–C**), ADC values (**D–F**), and ^{18}FET intensity (**G–I**). Cut-offs for Kaplan–Meier curves were determined by ROC curve analyses and depict patients in the bevacizumab (BEV) plus radiotherapy arm (**A, D, G**) and in the radiotherapy arm (**B, E, H**). HRs of indicated imaging parameters were determined for the entire cohort, interaction testing with treatment (interact bevacizumab) and treatment arms utilizing the Cox proportional hazards method (**C, F, I**). Contrast-enhancing tumor volume was analyzed as continuously scaled variable depicting the hazard per cm^3, ADC and ^{18}FET intensity values were dichotomized by ROC cut-offs.

(cut-off 55% contrast-enhancing volume reduction, median overall survival no response vs. response = 9.7 vs. 12.9 months, time-dependent $P = 0.023$; Supplementary Fig. S3D) than in the radiotherapy arm (cut-off 10% contrast-enhancing volume reduction, median overall survival no response vs. response = 8.9 vs. 14.4 months, time-dependent $P = 0.003$; Supplementary Fig. S3E). No associations with overall survival were observed for percent changes of T2 in either treatment arm (not shown).

^{18}FET-TBR of noncontrast-enhancing lesions is associated with overall survival in bevacizumab-treated patients

^{18}FET-PET was implemented in the ARTE trial to enable detection and monitoring of noncontrast-enhancing tumor burden in areas where antiangiogenic therapy has led to a tightened blood–brain barrier that prohibits contrast diffusion. Passive tracer diffusion into contrast-enhancing tumor portions (34) implies that the analysis of a metabolic response in either compartment is challenged by effects of bevacizumab on the spatial contrast-enhancing distribution. Comparing ^{18}FET-TBR of noncontrast-enhancing tumor portions to the identical tumor region that was contrast-enhancing before bevacizumab exposure will likely measure a decreased ^{18}FET intensity that may not reflect tumor cell death. As a surrogate for tumor burden and metabolic response to treatment in each compartment, we annotated ^{18}FET-TBR from first follow-up after radiotherapy (week 7) until progression in each patient. In patients with decreasing ^{18}FET-TBR at any time during follow-up, we utilized the lowest recorded follow-up value and in patients with increasing ^{18}FET-TBR, we utilized the highest recorded value to define a high versus low ^{18}FET-TBR cutoff by

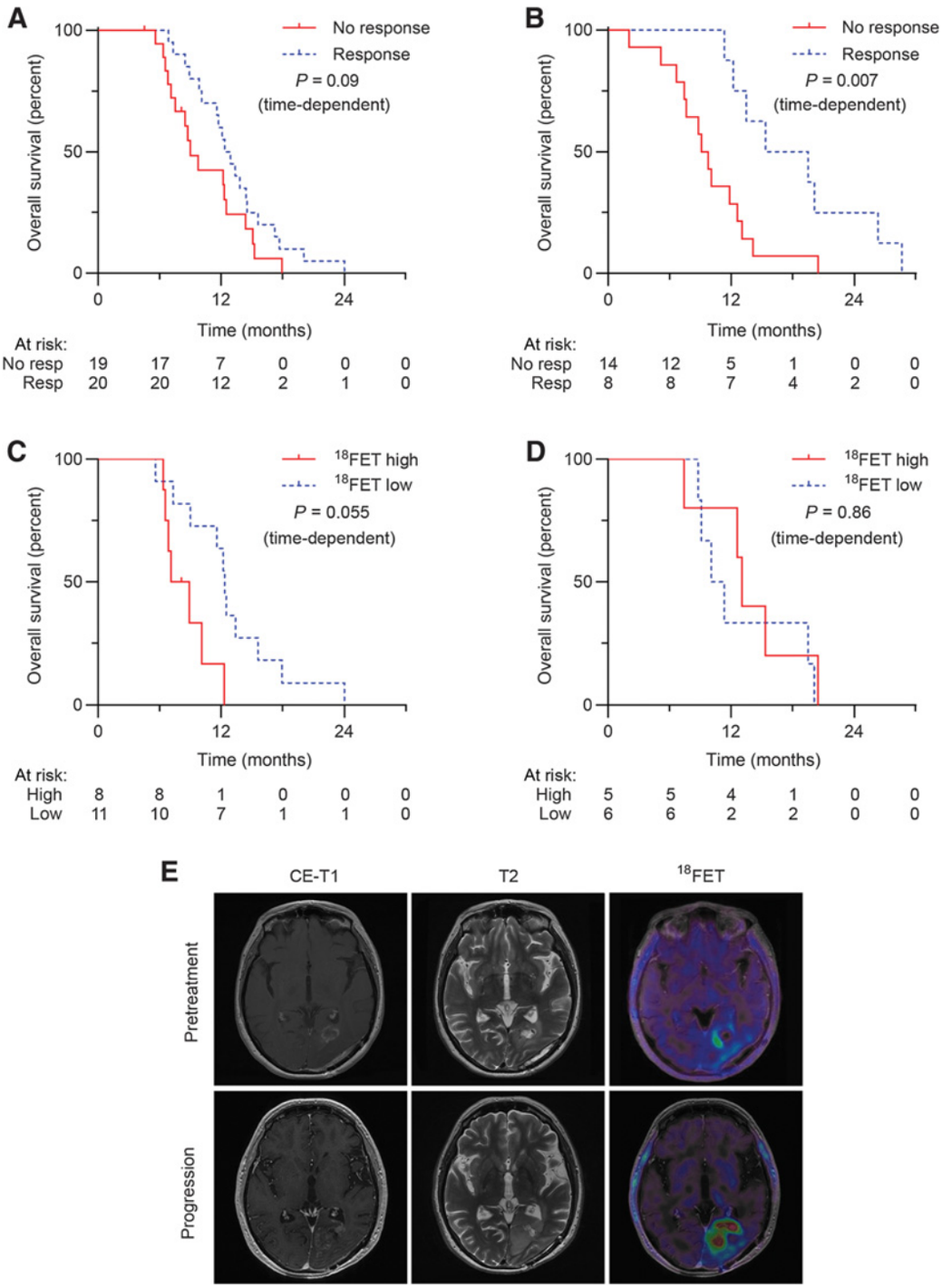

Figure 3.

Overall survival by MRI and PET response. Overall survival by best response classified as response versus no response at any time point until progression determined by the RANO criteria in the bevacizumab plus radiotherapy arm (**A**) and in the radiotherapy alone arm (**B**). Overall survival by best metabolic response classified as high versus low ^{18}FET-TBR of noncontrast-enhancing tumor portions at any time point posttreatment until progression in the bevacizumab plus radiotherapy arm (**C**) and in the radiotherapy alone arm (**D**); ^{18}FET-TBR cut-offs were determined by ROC curve analysis; overall survival of patients with high versus low ^{18}FET-TBR was compared by the Cox proportional hazards method computing best response as a time-dependent variable. **E,** Example of indicated imaging parameters before treatment and at progression; ^{18}FET-PET confirms tumor progression within non-CE-T1, T2 hyperintense regions; CE-T1, contrast enhancement on T1-weighted MRI sequences.

ROC curve analysis. In the bevacizumab plus radiotherapy arm, high ^{18}FET-TBR in noncontrast-enhancing tumor portions during follow-up after radiotherapy was associated with inferior overall survival by trend (**Fig. 3C**), but no such association was identified in the radiotherapy arm (**Fig. 3D**). Vice versa, high ^{18}FET-TBR in contrast-enhancing tumor portions during follow-up after radiotherapy was associated with overall survival in the radiotherapy arm only (Supplementary Fig. S4). An example of contrast enhancement, T2 and utilizing ^{18}FET PET is provided in **Fig. 3E**.

Imaging response by molecular subtypes

We also explored whether distinctive molecular glioblastoma subtypes defined by gene methylation, gene expression, or genomic copy-number alterations were enriched for response by RANO criteria or for high or low ^{18}FET-TBR in noncontrast-enhancing tumor during bevacizumab therapy. No such association was identified for complete or partial response versus stable disease or no response by RANO (not shown) and likewise, no association of high or low ^{18}FET-TBR in noncontrast-enhancing tumor was identified with gene methylation ($P = 0.38$), gene expression ($P = 0.37$), or genomic copy-number subtypes ($P = 0.29$).

Multivariate analyses

We sought to also explore imaging parameters associated with benefit from bevacizumab in a multivariate Cox regression model of overall survival that takes established prognostic factors into account, including age, KPS, and steroid intake. Univariate associations of these parameters with overall survival are summarized in Supplementary Table S3. Pretreatment contrast-enhancing tumor and ADC were both associated with overall survival (**Table 2**). We also identified an association of ADC_L with overall survival in this model (ADC_L HR per 0.1 mm/s^2 = 1.59; 95% CI, 1.04–2.43; $P = 0.033$). Follow-up imaging parameters at the first study visit after radiotherapy (week 7) were explored in this multivariate model as a clinically relevant paradigm of treatment reevaluation. There was a weak association of a decrease in contrast-enhancing tumor mass with improved overall survival. High noncontrast-enhancing ^{18}FET intensities on a single scan at first follow-up was associated with markedly inferior overall survival, suggesting that pseudoresponse was a negative predictor of overall survival. MGMT promotor methylation status was not associated with overall survival on univariate or multivariate analyses and had no relevant effect on HR determined for ADC or ^{18}FET intensities at baseline or at the first study visit after radiotherapy (not shown).

Table 2. Multivariate analysis of predictors of inferior overall survival.

Model	HR and 95% CI	*P*
Study arm: BEV plus RT vs. RT	0.78 (0.44–1.37)	0.39
Age: 65–70 years vs. >70 years	0.46 (0.27–0.78)	0.004
KPS: 90–100% vs. 60–80%	0.62 (0.35–1.09)	0.098
Steroids at study entry: no vs. yes	0.86 (0.56–1.42)	0.56
Imaging parameters[a]		
Baseline		
Contrast enhancement (per cm^3)	1.07 (1.01–1.13)	0.017
ADC (per 0.1 mm/s^2)	1.43 (1.04–1.98)	0.030
First follow-up (post-RT, Week 7)		
Contrast enhancement (per 10% response)	0.97 (0.95–0.99)	0.021
^{18}FET intensity in noncontrast-enhancing tumor portions (high vs. low)[b]	5.97 (1.16–30.8)	0.033

Abbreviation: BEV, bevacizumab.

[a]Adjusted for interaction with study arm and tested as additional single variables.

[b]Cutoffs defined by ROC curve analyses; univariate analyses are summarized in Supplementary Table S3.

Discussion

The present secondary analyses of the randomized ARTE trial explored MRI- and PET-based parameters for selection and monitoring of patients with newly diagnosed IDH wild-type glioblastoma during bevacizumab therapy.

Pretreatment MRI parameters including contrast-enhancing tumor and ADC, but not T2 volumes stratified bevacizumab plus radiotherapy-treated patients by overall survival and were associated with specific benefit from bevacizumab plus radiotherapy compared with radiotherapy alone. There was also a strong association of pretreatment ^{18}FET intensities in contrast-enhancing tumor with overall survival, but this was not specific for the bevacizumab plus radiotherapy arm.

The interaction of larger pretreatment contrast-enhancing volume with preferential overall survival benefit from bevacizumab plus radiotherapy is supported by a less pronounced association of pretreatment tumor size with overall survival in the bevacizumab plus radiotherapy arm than in the radiotherapy arm. Similar results by trend have also been reported from the phase III AVAglio trial of bevacizumab in combination with chemoradiotherapy versus chemoradiotherapy alone in newly diagnosed glioblastoma (36). Other factors such as temozolomide treatment and *MGMT* promoter methylation status may have been more important prognostic factors in AVAglio than in ARTE.

Extent of resection was not determined in the ARTE cohort. However, a relevant association of smaller postoperative contrast-enhanced tumor volume with longer overall survival was noted in both treatment arms, supporting maximum safe resection as the standard of care irrespective of whether or not bevacizumab is administered (37).

The phase III European Organization for Research and Treatment of Cancer (EORTC) 26101 trial assessed the efficacy of bevacizumab in combination with lomustine in recurrent glioblastoma (6). Our study expands on *post hoc* analyses of this trial in the newly diagnosed setting by confirming an association of baseline imaging necrosis with inferior overall survival (11). A dynamic increase of imaging necrosis during treatment was observed in a small proportion of patients in EORTC 26101 and, irrespective of treatment (11). Similar analyses of outcome by dynamics of necrosis were not feasible in the ARTE study due to the relatively smaller sample size. In the EORTC 26101 cohort, presence of necrosis also predicted inferior survival of the bevacizumab plus lomustine arm compared with the lomustine alone arm (11), but a similar association of bevacizumab plus radiotherapy was not noted in the ARTE cohort.

Our study also supports retrospective studies and reports from uncontrolled clinical trials in recurrent glioblastoma that proposed ADC as a prognostic parameter in patients treated with bevacizumab (9, 10, 38). As a potential limitation and in contrast to these previous studies, we have however used mean ADC and not a double Gaussian mixed model for most analyses. Nonetheless, the randomized design of our study supports that ADC may be predictive of benefit from bevacizumab rather than a treatment-agnostic prognostic factor.

The rationale for the use of amino acid PET in patients treated with bevacizumab is to identify and monitor viable noncontrast-enhancing tumor portions to account for a commonly observed reduction of

contrast enhancement that does not necessarily reflect tumor cell death (17, 24). The clinical utility of this rationale was supported by a strong negative association of noncontrast-enhancing ^{18}FET intensity with overall survival specifically in patients treated with bevacizumab plus radiotherapy. This association was confirmed on multivariate analyses at first follow-up after radiotherapy, suggesting that amino acid PET may serve as an early marker of pseudoresponse and as a predictor of overall survival benefit during bevacizumab plus radiotherapy treatment. In contrast, the similar ^{18}FET intensity of normal brain and noncontrast-enhancing tumor before treatment or post-radiotherapy in the radiotherapy arm suggest that the majority of hyperintensity on T2-weighted MRI represents vasogenic edema. Our findings support the proposal by the RANO working group to utilize amino acid PET to monitor tumor growth in bevacizumab-treated patients with glioblastoma and complements feasibility studies that have indicated better accuracy of amino acid PET for disease monitoring than conventional MRI in bevacizumab-treated patients with glioma (20, 22, 39–42). However, the small sample size of the PET cohort warrants further validation of amino acid PET as a predictor of overall survival during antiangiogenic therapy.

The lack of overall survival association of T2 pretreatment volumes or dynamics in either treatment arm of ARTE is of note given that part of the rationale to include a T2-based definition of progression in the RANO criteria was to account for pseudoresponse to antiangiogenic therapy (12). Our findings underscore that dynamics of T2 hyperintensity do not generally reflect the disease course, but require careful evaluation in the context of clinical assessments and treatment. For example, a T2 "response" may simply reflect regression of edema in response to bevacizumab, and *vice versa* T2 "progression" may reflect an increase of edema when steroids are weaned, or delayed radiation effects. Along the same lines, response defined by the contrast enhancement- and T2-based RANO criteria were only weakly associated with overall survival in this study and in AVAglio (19).

The lack of overall survival benefit in phase III clinical trials of bevacizumab in combination with standard treatments in newly diagnosed (7, 8) and recurrent glioblastoma (6) may be considered at odds with reports of imaging biomarkers that have been proposed to identify patients with presumed overall survival benefit from bevacizumab. If subgroups of patients derive overall survival benefit, other subgroups will experience harm from bevacizumab when the net outcome is neutral.

A possible interpretation may be that the herein reported association of higher ^{18}FET-TBR in noncontrast-enhancing tumor portions with inferior overall survival reflects delayed diagnosis of progression and thus deferred salvage therapy. The considerably smaller proportion of patients in the bevacizumab plus radiotherapy arm compared with the radiotherapy arm who received any salvage treatment in ARTE (first salvage therapy 25/50 = 50% vs. 18/25 = 72%, second salvage therapy 7/50 = 14% vs. 14/25 = 56%; ref. 25) supports this explanation. Along the same lines, interobserver bias with respect to the diagnosis of progression by RANO criteria has been reported from several clinical trials with central radiology review, including ARTE (25) and EORTC 26101 (6, 18). Albeit not statistically amenable, differences in assessment and outcome between the two phase III clinical trials of bevacizumab in newly diagnosed glioblastoma also support the notion that deferred diagnosis of progression may negatively impact overall survival in patients treated with bevacizumab. The contrast enhancement-based Macdonald criteria (13) in the RTOG 0825 trial and the RANO criteria (12) in the AVAglio trial conveyed HRs for bevacizumab of 1.12 and 0.88, respectively (7, 8). However, the fact that the vast majority of patients in the ARTE trial had an unmethylated MGMT promoter questions whether the limited efficacy of temozolomide or lomustine in a recurrent setting would have yielded a clinically relevant difference in overall survival.

Strengths of our study include the thorough annotation of clinical, molecular, and imaging parameters. The statistical power was likely further enhanced by the inclusion of only elderly patients, because this patient population is deemed to preferentially benefit from bevacizumab in combination with different chemotherapy regimens based on early uncontrolled trials (5, 43, 44). Moreover, confounding factors were reduced by exclusion of patients with IDH-mutated glioblastoma, which was defined as a distinct entity in the current World Health Organization (WHO) classification of primary brain tumors based on molecular and clinical features distinct from the majority of glioblastomas that lack IDH mutations (2). Other poor prognostic characteristics of the ARTE cohort include the lack of *MGMT* promoter methylation in the large majority of patients, because patients with methylated *MGMT* promoter were excluded from ARTE by amendment when it became clear that these patients would derive more benefit from temozolomide than from radiotherapy (37). That *MGMT* promoter methylation was not prognostic in the ARTE trial is explained by the fact that the patients did not receive first-line temozolomide and that only few patients received alkylating chemotherapy at recurrence.

Limitations of the analysis include its relatively small sample size, particularly in the PET cohort. Although the ARTE trial was designed to include a poor prognosis population—i.e., elderly patients with unmethylated MGMT—the median overall survival of approximately 12 months is considerably longer than expected on the basis of epidemiologic studies (1, 45). Reasons for this apparent selection of patients with better prognostic traits include that patients were required to be able to travel every other week to receive bevacizumab infusions. The optional participation in the PET study of the ARTE trial required additional traveling and may have aggravated the selection toward patients in a better clinical condition. However, patient characteristics and overall survival were similar in the MRI and PET cohorts, thus arguing against relevant selection bias between these groups.

Another limitation of our study is that bevacizumab is not commonly used in the newly diagnosed setting of the ARTE trial, but mostly at recurrence of glioblastoma. Beyond amino acid PET, the dramatic progress and clinical implementation of advanced MRI technologies warrants the expansion of multimodal imaging for monitoring of glioblastomas, for example, by MR spectroscopy (46) or perfusion imaging (47). Finally, the clinical feasibility of machine learning algorithms to define response and progression has been demonstrated in the context of bevacizumab therapy of glioblastoma (18, 48), supporting that unbiased approaches may aid in integrating large amounts of data from multimodal imaging in future studies.

In summary, we provide a comprehensive validation of current imaging standards and propose improvements in the context of bevacizumab treatment of glioblastoma. Our study falsifies T2 as a relevant marker of tumor growth during bevacizumab treatment and does not unambiguously support patient selection for bevacizumab treatment based on higher ADC, but supports the preferential use of bevacizumab in patients with larger contrast-enhancing volumes, and the use of amino acid PET to monitor antiangiogenic treatment (24). Future studies applying these and other parameters prospectively are warranted to improve patient selection and disease monitoring in patients treated with bevacizumab, particularly in the recurrent setting for which bevacizumab has obtained clinical approval in the United States and other countries.

Authors' Disclosures

H.-G. Wirsching reports grants and personal fees from F. Hoffmann-La Roche during the conduct of the study. T. Hundsberger reports grants from Clinical trial unit commission, cantonal hospital St. Gallen (academic grant) during the conduct of the study. A.F. Hottinger reports grants and other from Novocure (paid to institution) outside the submitted work. R. von Moos reports personal fees from Roche (advisory board participant) and MSD (advisory board participant) during the conduct of the study. P. Roth reports grants from MSD and Novocure; personal fees from Bristol-Myers Squibb, Debiopharm, Medac, Merck, QED, Virometix, and Roche outside the submitted work. G. Tabatabai reports personal fees from Roche and grants from Roche Diagnostics during the conduct of the study; personal fees from Bayer, personal fees and nonfinancial support from AbbVie, and grants and personal fees from Novocure and Medac outside the submitted work. M. Weller reports grants from Roche during the conduct of the study; grants and personal fees from Abbvie and MSD, grants from Adastra and Novocure, personal fees from Roche, Merck (EMD), Basilea, Orbus, Nerviano, Tocagen, Celgene, Medac, and Philogen outside the submitted work. No disclosures were reported by the other authors.

Authors' Contributions

H.-G. Wirsching: Conceptualization, data curation, formal analysis, investigation, visualization, methodology, writing-original draft, project administration, writing-review and editing. **U. Roelcke:** Data curation, investigation, methodology. **J. Weller:** Data curation, software, investigation. **T. Hundsberger:** Investigation. **A.F. Hottinger:** Investigation. **R. von Moos:** Investigation. **F. Caparrotti:** Investigation. **K. Conen:** Investigation. **L. Remonda:** Investigation. **P. Roth:** Investigation. **A. Ochsenbein:** Investigation. **G. Tabatabai:** Investigation, project administration. **M. Weller:** Conceptualization, resources, supervision, funding acquisition, validation, investigation, methodology, writing-original draft, project administration, writing-review and editing.

Acknowledgments

The ARTE trial was supported by a grant from F. Hoffmann-La Roche. H.-G. Wirsching was supported by a grant from the University Hospital Zurich (Zurich, Switzerland).

The costs of publication of this article were defrayed in part by the payment of page charges. This article must therefore be hereby marked *advertisement* in accordance with 18 U.S.C. Section 1734 solely to indicate this fact.

Received May 29, 2020; revised August 9, 2020; accepted September 17, 2020; published first September 23, 2020.

References

1. Ostrom QT, Cioffi G, Gittleman H, Patil N, Waite K, Kruchko C, et al. CBTRUS statistical report: primary brain and other central nervous system tumors diagnosed in the United States in 2012–2016. Neuro Oncol 2019;21:v1–v100.
2. Louis DN, Perry A, Reifenberger G, von Deimling A, Figarella-Branger D, Cavenee WK, et al. The 2016 world health organization classification of tumors of the central nervous system: a summary. Acta Neuropathol 2016;131:803–20.
3. Presta LG, Chen H, O'Connor SJ, Chisholm V, Meng YG, Krummen L, et al. Humanization of an anti-vascular endothelial growth factor monoclonal antibody for the therapy of solid tumors and other disorders. Cancer Res 1997;57:4593–9.
4. Friedman HS, Prados MD, Wen PY, Mikkelsen T, Schiff D, Abrey LE, et al. Bevacizumab alone and in combination with irinotecan in recurrent glioblastoma. J Clin Oncol 2009;27:4733–40.
5. Kreisl TN, Kim L, Moore K, Duic P, Royce C, Stroud I, et al. Phase II trial of single-agent bevacizumab followed by bevacizumab plus irinotecan at tumor progression in recurrent glioblastoma. J Clin Oncol 2009;27:740–5.
6. Wick W, Gorlia T, Bendszus M, Taphoorn M, Sahm F, Harting I, et al. Lomustine and bevacizumab in progressive glioblastoma. N Engl J Med 2017;377:1954–63.
7. Chinot OL, Wick W, Mason W, Henriksson R, Saran F, Nishikawa R, et al. Bevacizumab plus radiotherapy-temozolomide for newly diagnosed glioblastoma. N Engl J Med 2014;370:709–22.
8. Gilbert MR, Dignam JJ, Armstrong TS, Wefel JS, Blumenthal DT, Vogelbaum MA, et al. A randomized trial of bevacizumab for newly diagnosed glioblastoma. N Engl J Med 2014;370:699–708.
9. Ellingson BM, Sahebjam S, Kim HJ, Pope WB, Harris RJ, Woodworth DC, et al. Pretreatment ADC histogram analysis is a predictive imaging biomarker for bevacizumab treatment but not chemotherapy in recurrent glioblastoma. AJNR Am J Neuroradiol 2014;35:673–9.
10. Ellingson BM, Gerstner ER, Smits M, Huang RY, Colen R, Abrey LE, et al. Diffusion MRI phenotypes predict overall survival benefit from anti-VEGF monotherapy in recurrent glioblastoma: converging evidence from phase II trials. Clin Cancer Res 2017;23:5745–56.
11. Nowosielski M, Gorlia T, Bromberg JEC, Sahm F, Harting I, Kickingereder P, et al. Imaging necrosis during treatment is associated with worse survival in EORTC 26101 study. Neurology 2019;92:e2754–e63.
12. Wen PY, Macdonald DR, Reardon DA, Cloughesy TF, Sorensen AG, Galanis E, et al. Updated response assessment criteria for high-grade gliomas: response assessment in neuro-oncology working group. J Clin Oncol 2010;28:1963–72.
13. Macdonald DR, Cascino TL, Schold SC Jr, Cairncross JG. Response criteria for phase II studies of supratentorial malignant glioma. J Clin Oncol 1990;8:1277–80.
14. Batchelor TT, Sorensen AG, di Tomaso E, Zhang WT, Duda DG, Cohen KS, et al. AZD2171, a pan-VEGF receptor tyrosine kinase inhibitor, normalizes tumor vasculature and alleviates edema in glioblastoma patients. Cancer Cell 2007;11:83–95.
15. Nowosielski M, Wiestler B, Goebel G, Hutterer M, Schlemmer HP, Stockhammer G, et al. Progression types after antiangiogenic therapy are related to outcome in recurrent glioblastoma. Neurology 2014;82:1684–92.
16. Reardon DA, Ballman KV, Buckner JC, Chang SM, Ellingson BM. Impact of imaging measurements on response assessment in glioblastoma clinical trials. Neuro Oncol 2014;16Suppl 7:vii24–35.
17. Brandsma D, van den Bent MJ. Pseudoprogression and pseudoresponse in the treatment of gliomas. Curr Opin Neurol 2009;22:633–8.
18. Kickingereder P, Isensee F, Tursunova I, Petersen J, Neuberger U, Bonekamp D, et al. Automated quantitative tumour response assessment of MRI in neuro-oncology with artificial neural networks: a multicentre, retrospective study. Lancet Oncol 2019;20:728–40.
19. Ellingson BM, Abrey LE, Garcia J, Chinot O, Wick W, Saran F, et al. Post-chemoradiation volumetric response predicts survival in newly diagnosed glioblastoma treated with radiation, temozolomide, and bevacizumab or placebo. Neuro Oncol 2018;20:1525–35.
20. Galldiks N, Dunkl V, Ceccon G, Tscherpel C, Stoffels G, Law I, et al. Early treatment response evaluation using FET PET compared to MRI in glioblastoma patients at first progression treated with bevacizumab plus lomustine. Eur J Nucl Med Mol Imaging 2018;45:2377–86.
21. de Zwart PL, van Dijken BR, Holtman GA, Stormezand GN, Dierckx RA, van Laar PJ, et al. Diagnostic accuracy of positron emission tomography tracers for the differentiation of tumor progression from treatment-related changes in high-grade glioma: a systematic review and meta-analysis. J Nucl Med 2019;61:498–504.
22. Galldiks N, Rapp M, Stoffels G, Fink GR, Shah NJ, Coenen HH, et al. Response assessment of bevacizumab in patients with recurrent malignant glioma using [18F]Fluoroethyl-L-tyrosine PET in comparison to MRI. Eur J Nucl Med Mol Imaging 2013;40:22–33.
23. Hutterer M, Nowosielski M, Putzer D, Waitz D, Tinkhauser G, Kostron H, et al. O-(2–18F-fluoroethyl)-L-tyrosine PET predicts failure of antiangiogenic treatment in patients with recurrent high-grade glioma. J Nucl Med 2011;52:856–64.
24. Albert NL, Weller M, Suchorska B, Galldiks N, Soffietti R, Kim MM, et al. Response assessment in neuro-oncology working group and european association for neuro-oncology recommendations for the clinical use of PET imaging in gliomas. Neuro Oncol 2016;18:1199–208.
25. Wirsching HG, Tabatabai G, Roelcke U, Hottinger AF, Jorger F, Schmid A, et al. Bevacizumab plus hypofractionated radiotherapy versus radiotherapy alone in elderly patients with glioblastoma: the randomized, open-label, phase II ARTE trial. Ann Oncol 2018;29:1423–30.
26. Malmstrom A, Gronberg BH, Marosi C, Stupp R, Frappaz D, Schultz H, et al. Temozolomide versus standard 6-week radiotherapy versus hypofractionated radiotherapy in patients older than 60 years with glioblastoma: the Nordic randomised, phase 3 trial. Lancet Oncol 2012;13:916–26.

27. Wick W, Platten M, Meisner C, Felsberg J, Tabatabai G, Simon M, et al. Temozolomide chemotherapy alone versus radiotherapy alone for malignant astrocytoma in the elderly: the NOA-08 randomised, phase 3 trial. Lancet Oncol 2012;13:707–15.
28. Felsberg J, Rapp M, Loeser S, Fimmers R, Stummer W, Goeppert M, et al. Prognostic significance of molecular markers and extent of resection in primary glioblastoma patients. Clin Cancer Res 2009;15:6683–93.
29. Capper D, Zentgraf H, Balss J, Hartmann C, von Deimling A. Monoclonal antibody specific for IDH1 R132H mutation. Acta Neuropathol (Berl) 2009;118: 599–601.
30. Capper D, Jones DTW, Sill M, Hovestadt V, Schrimpf D, Sturm D, et al. DNA methylation-based classification of central nervous system tumours. Nature 2018;555:469–74.
31. Cimino PJ, Zager M, McFerrin L, Wirsching HG, Bolouri H, Hentschel B, et al. Multidimensional scaling of diffuse gliomas: application to the 2016 World Health Organization classification system with prognostically relevant molecular subtype discovery. Acta Neuropathol Commun 2017;5:39.
32. Sandmann T, Bourgon R, Garcia J, Li C, Cloughesy T, Chinot OL, et al. Patients with proneural glioblastoma may derive overall survival benefit from the addition of bevacizumab to first-line radiotherapy and temozolomide: retrospective analysis of the AVAglio trial. J Clin Oncol 2015;33:2735–44.
33. Verhaak RG, Hoadley KA, Purdom E, Wang V, Qi Y, Wilkerson MD, et al. Integrated genomic analysis identifies clinically relevant subtypes of glioblastoma characterized by abnormalities in PDGFRA, IDH1, EGFR, and NF1. Cancer Cell 2010;17:98–110.
34. Hutterer M, Nowosielski M, Putzer D, Jansen NL, Seiz M, Schocke M, et al. [18F]-fluoro-ethyl-L-tyrosine PET: a valuable diagnostic tool in neuro-oncology, but not all that glitters is glioma. Neuro Oncol 2013;15:341–51.
35. Roelcke U, Wyss MT, Nowosielski M, Ruda R, Roth P, Hofer S, et al. Amino acid positron emission tomography to monitor chemotherapy response and predict seizure control and progression-free survival in WHO grade II gliomas. Neuro Oncol 2016;18:744–51.
36. Ellingson BM, Abrey LE, Nelson SJ, Kaufmann TJ, Garcia J, Chinot O, et al. Validation of postoperative residual contrast-enhancing tumor volume as an independent prognostic factor for overall survival in newly diagnosed glioblastoma. Neuro Oncol 2018;20:1240–50.
37. Weller M, van den Bent M, Tonn JC, Stupp R, Preusser M, Cohen-Jonathan-Moyal E, et al. European Association for Neuro-Oncology (EANO) guideline on the diagnosis and treatment of adult astrocytic and oligodendroglial gliomas. Lancet Oncol 2017;18:e315–e29.
38. Pope WB, Qiao XJ, Kim HJ, Lai A, Nghiemphu P, Xue X, et al. Apparent diffusion coefficient histogram analysis stratifies progression-free and overall survival in patients with recurrent GBM treated with bevacizumab: a multi-center study. J Neurooncol 2012;108:491–8.
39. Harris RJ, Cloughesy TF, Pope WB, Nghiemphu PL, Lai A, Zaw T, et al. 18F-FDOPA and 18F-FLT positron emission tomography parametric response maps predict response in recurrent malignant gliomas treated with bevacizumab. Neuro Oncol 2012;14:1079–89.
40. Galldiks N, Rapp M, Stoffels G, Dunkl V, Sabel M, Langen KJ. Earlier diagnosis of progressive disease during bevacizumab treatment using O-(2–18F-fluorethyl)-L-tyrosine positron emission tomography in comparison with magnetic resonance imaging. Mol Imaging 2013;12:273–6.
41. Deuschl C, Moenninghoff C, Goericke S, Kirchner J, Koppen S, Binse I, et al. Response assessment of bevacizumab therapy in GBM with integrated 11C-MET-PET/MRI: a feasibility study. Eur J Nucl Med Mol Imaging 2017;44:1285–95.
42. George E, Kijewski MF, Dubey S, Belanger AP, Reardon DA, Wen PY, et al. Voxel-wise analysis of fluoroethyltyrosine PET and MRI in the assessment of recurrent glioblastoma during antiangiogenic therapy. AJR Am J Roentgenol 2018;211:1342–7.
43. Nghiemphu PL, Liu W, Lee Y, Than T, Graham C, Lai A, et al. Bevacizumab and chemotherapy for recurrent glioblastoma: a single-institution experience. Neurology 2009;72:1217–22.
44. Lai A, Tran A, Nghiemphu PL, Pope WB, Solis OE, Selch M, et al. Phase II study of bevacizumab plus temozolomide during and after radiation therapy for patients with newly diagnosed glioblastoma multiforme. J Clin Oncol 2011; 29:142–8.
45. Gramatzki D, Dehler S, Rushing EJ, Zaugg K, Hofer S, Yonekawa Y, et al. Glioblastoma in the canton of zurich, Switzerland revisited: 2005 to 2009. Cancer 2016;122:2206–15.
46. Hattingen E, Jurcoane A, Bahr O, Rieger J, Magerkurth J, Anti S, et al. Bevacizumab impairs oxidative energy metabolism and shows antitumoral effects in recurrent glioblastomas: a 31P/1H MRSI and quantitative magnetic resonance imaging study. Neuro Oncol 2011;13:1349–63.
47. Kickingereder P, Radbruch A, Burth S, Wick A, Heiland S, Schlemmer HP, et al. MR perfusion-derived hemodynamic parametric response mapping of bevacizumab efficacy in recurrent glioblastoma. Radiology 2016;279:542–52.
48. Chang K, Zhang B, Guo X, Zong M, Rahman R, Sanchez D, et al. Multimodal imaging patterns predict survival in recurrent glioblastoma patients treated with bevacizumab. Neuro Oncol 2016;18:1680–7.